

# State-specific photofragment yield spectroscopy of jet-cooled methyl nitrite

S.A. Reid, J.T. Brandon and H. Reisler

*Department of Chemistry, University of Southern California, Los Angeles, CA 90089-0482, USA*

Received 29 March 1993; in final form 26 April 1993

We obtained state-specific photofragment yield (PHOFRY) spectra of jet-cooled  $\text{CH}_3\text{ONO}$  in the  $S_1 \leftarrow S_0$  absorption system by monitoring selected rotational levels in  $\text{NO } \nu=0, 1$  and  $2$ . The spectra exhibit bands which are assigned to both the syn- and anti-rotamers with origins at 380 nm and 388 nm, respectively. All the bands are broad ( $500\text{--}800 \text{ cm}^{-1}$ ) suggesting that the dissociation lifetimes are shorter than those obtained in dynamical calculations on model potential energy surfaces. The widths do not depend on the monitored  $\text{NO}$  rotational level. The results support a mechanism where nonadiabatic vibrational predissociation is preferred.

## 1. Introduction

The photodissociation of molecules of the form  $\text{RNO}$  ( $\text{R}=\text{HO}, \text{CH}_3\text{O}, \text{Cl}, \text{F}$ , etc.) has been the subject of numerous experimental and theoretical investigations [1–3]. Most of these molecules show diffuse vibronic structure in their 300 K  $S_1 \leftarrow S_0$  electronic spectra and their dissociation can be described as



where  $[\text{RNO}]^{\ddagger}$  denotes the transition state. In particular, the photodissociation of methyl nitrite ( $\text{CH}_3\text{ONO}$ ) has been studied in great detail both experimentally and theoretically [4–17], and in addition has been the object of numerous spectroscopic studies [18–21], which have determined that both syn- and anti-rotameric forms are present in the gas phase at room temperature. Studies of the temperature dependence of infrared band intensities have shown that the energy difference between the more stable syn- (stabilized by intramolecular hydrogen bonding) and anti-rotamers is  $219 \text{ cm}^{-1}$  in the ground electronic state [19], implying a gas-phase room temperature conformational population distribution  $n_{\text{syn}}/n_{\text{anti}}=1.8$ .

The electronic spectroscopy of methyl nitrite has been the subject of several investigations [9,20,21].

At room temperature, the  $S_1 \leftarrow S_0$  absorption system exhibits a series of broad features spaced by  $\approx 1000 \text{ cm}^{-1}$  (fig. 1), assigned as a long progression in the  $\text{N}=\text{O}$  stretching mode ( $3\nu_2^{\text{NO}}$ ) [21]. Due both to superposition of the band systems of the two rotamers and inhomogeneous broadening, the band assignments in this system have not been unambiguously determined. Tarte [21] assigned the longest wavelength feature observed at  $\approx 387 \text{ nm}$  to the origin of the anti-system, with the syn-origin placed at  $\approx 381 \text{ nm}$ . The most intense features at shorter wavelengths were assigned to the  $\text{NO}$ -stretch progression members of the syn-system. This assignment, however, has recently come into question (see below) [22–24].

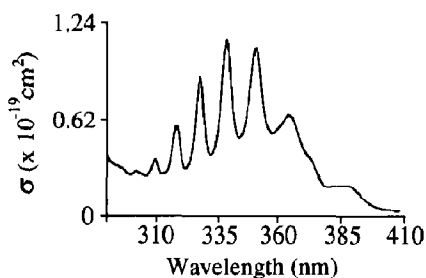


Fig. 1. 300 K absorption spectrum of methyl nitrite ( $S_1 \leftarrow S_0$ ), obtained with 50 Torr of purified  $\text{CH}_3\text{ONO}$  and a path length of  $\approx 10 \text{ cm}$ .

Product state distributions of the NO fragment following excitation into various bands of the  $S_1$  system have been obtained under both jet-cooled and 300 K conditions [9,10,15,16,25]. The rotational distributions obtained at all wavelengths have the same form – Gaussian in shape and peaking at high  $J$  values (i.e.  $J > 30.5$ ) [15]. These distributions are well fit by a rotational reflection model that incorporates mapping of the parent excited-state bending wavefunction mediated by the exit-channel interactions. The latter are strong as evidenced by the high level of rotational excitation [1,5,13]. In addition, the vibrational distributions obtained following excitation into  $3_0^+$  bands of the syn-rotamer (Tarte assignment [21]) show a marked preference for populating the  $(n-1)$  vibrational level of the NO fragment [10,16,25]. This has been interpreted as preference for a vibrationally nonadiabatic predissociation mechanism, in which loss of one quantum of NO vibration through vibrational–translational coupling results in dissociation on the lower vibrationally adiabatic surface of the  $S_1$  state [5,13]. The observed vibrational distributions have been reasonably well fit theoretically using a potential energy surface (PES) calculated in only two degrees of freedom ( $r_{N-O}$  and  $R_{O-N}$ ), with the bending angle frozen [5]. More recent 3D wave-packet calculations, which incorporate also the O–N=O bending angle, give yet better agreement with the measured vibrational and rotational distributions [13].

An important aspect of the comparisons between theory and experiment involves the absorptions linewidths, which are related to the dissociation lifetimes. The most recent calculations predict lifetimes of 200–300 fs, depending on the  $S_1$  vibronic level of the syn-rotamer, which correspond to a lifetime broadened contribution to the linewidth of  $\approx 15$ –25  $\text{cm}^{-1}$  [13]. The 300 K absorption spectrum exhibits much broader peaks ( $> 500 \text{ cm}^{-1}$ ), but the difference has been attributed to superposition of spectral features of the syn- and anti-rotamers and inhomogeneous thermal broadening. Indirect estimates of the linewidths, derived from measurements of the recoil anisotropy parameter  $\beta$ , are in better agreement with the theoretical predictions [17]. A direct measurement of the linewidths in jet-cooled spectra is clearly desirable for meaningful comparisons with theory.

In addition, we note that the Tarte assignments of the  $S_1 \leftarrow S_0$  absorption system [21] have recently been questioned. Based on changes in band intensities in this system with temperature in the range  $T=203$ –293 K, Hippler and co-workers have suggested a revised assignment which places the origin of the syn-rotamer at  $\lambda=363.9 \text{ nm}$  [22–24]. This assignment, if correct, would suggest that dissociation predominantly occurs through a vibrationally *adiabatic* mechanism (i.e.  $n^* \rightarrow n$ , where  $n^*$  denotes the NO-stretch resonance in  $S_1$  and  $n$  is the vibrational quantum number of NO), and therefore require severe revision of the theory. In our previous work, we have shown that state-specific photofragment yield (PHOFRY) spectra of fast-dissociating molecules can yield valuable information on spectra assignments and linewidths and, in addition, serve as sensitive probes of the dynamics [26]. Therefore, we have obtained PHOFRY spectra of methyl nitrite in the range  $\lambda=344$ –400 nm using jet-cooled samples, thereby significantly reducing the contributions of inhomogeneous broadening and allowing a better comparison with the calculated absorption spectrum [13]. The results reported here support a vibrationally nonadiabatic predissociation mechanism and the Tarte spectroscopic assignments [21], but show linewidths much broader than predicted by theory.

## 2. Experimental

The experimental apparatus and methodology have previously been described in detail [26,27]. Briefly, a mixture of  $\text{CH}_3\text{ONO}/\text{He}$  (typically 4%–9%) is expanded into an octagonal vacuum chamber (base pressure  $1 \times 10^{-6}$  Torr) using a piezoelectrically actuated pulsed nozzle (pulsewidth  $\approx 180 \mu\text{s}$ , orifice diameter = 0.5 mm) at typical stagnation pressures of 500–760 Torr. Under these expansion conditions, significant relaxation of the 300 K conformational distribution is not expected [19], nor is cluster formation [16]. Both syn- and anti-rotamers of methyl nitrite are dissociated  $\approx 15 \text{ mm}$  downstream of the orifice by one-photon excitation using an excimer-pumped tunable dye-laser system. Nascent NO fragments are probed at a photolysis-probe delay of 200 ns via laser-induced fluorescence (LIF) on the diagonal sequence bands of the well known  $\gamma$ -system

using a second excimer-pumped tunable dye-laser system, the output of which is frequency-doubled in a BBO crystal. The photolysis and probe beams are collinear and counterpropagating with parallel linear polarizations. The laser beams are polarized perpendicular to the axis of the solar blind PMT (Hamamatsu RU166H) employed for fluorescence detection, which is oriented orthogonally to both the molecular beam axis and the propagation axis of the laser beams. Fluorescence is imaged onto the PMT through a "solar blind" filter (Corion) using a three-lens telescope. The PMT signal is digitized by a digital storage oscilloscope and subsequently sent to a computer which controls data acquisition and laser frequency stepping.

State-specific PHOFRY spectra were obtained by fixing the probe laser frequency to excite a specific transition in a selected band of the NO  $\gamma$ -system and scanning the photolysis laser frequency to obtain a partial yield spectrum for dissociation into the monitored state. In these measurements, probe pulse energies of 10–40  $\mu$ J were used, since partial saturation of the strong NO transitions was not of concern. The probe beam was not focused but collimated to  $\approx$  5 mm diameter. The photolysis beam (3–11 mJ) was loosely focused to  $\approx$  2 mm diameter at the interaction region using a 1 m CaF<sub>2</sub> lens. The following dyes and dye combinations were used to cover the wavelength range 334–400 nm: QUI (400–370 nm), QUI/BPBD-365 (390–360 nm), BPBD-365 (370–358 nm), BPBD-365/Exalite 351 (368–353 nm), and Exalite 351 (358–344 nm). By using dye combinations we eliminated the increased amplified spontaneous emission (ASE) which can be quite severe at the edges of a single dye tuning curve. The LIF signals were normalized to both laser energies, and the different spectral segments were overlapped and smoothed to yield the composite PHOFRY spectra displayed in figs. 2 and 3. The smoothing does not alter the shapes of the bands.

Methyl nitrite was prepared in the standard manner by dropwise addition of dilute sulfuric acid (H<sub>2</sub>SO<sub>4</sub>) to a solution of sodium nitrite in aqueous methanol [28]. The resulting gas was collected in a liquid nitrogen cooled finger and purified by trap-to-trap distillation with an ice bath. FTIR and UV spectra of the purified sample were identical to the pub-

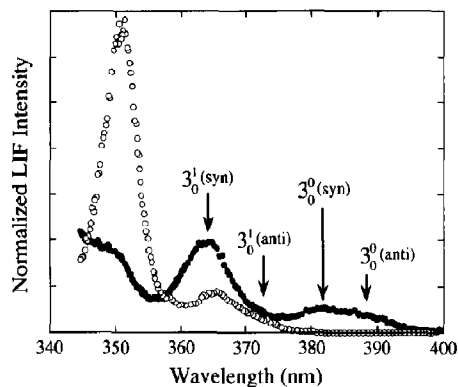


Fig. 2. State-specific photofragment yield (PHOFRY) spectra of methyl nitrite obtained by monitoring the  $Q_{22}(35.5)$  transitions in the (1, 1) and (0, 0) bands of the NO  $\gamma$ -system. The spectra are normalized at a single wavelength (363.9 nm) as described in the text, and the band assignments for the two rotamers are notated. (●) Probe NO( $\nu=0$ ); (○) probe NO( $\nu=1$ ).

lished spectra [18,21], and showed no evidence of HONO impurity.

### 3. Results and discussion

Relative partial absorption cross sections into specific NO( $\nu, J$ ) states were obtained by fixing the probe laser at specific bands of the  $\gamma$ -system and scanning the photolysis laser across several absorption features in the region 344–400 nm. Displayed in fig. 2 are two state-specific PHOFRY spectra obtained by monitoring the  $Q_{22}(35.5)$  transitions of the (0, 0) and (1, 1) bands of the NO  $\gamma$ -system. The PHOFRY spectra are normalized at a single wavelength ( $\lambda=363.9$  nm) to the NO rovibrational distributions recently obtained by Kades et al. under jet-cooled conditions [16]. Although the NO rotational and spin-orbit distributions obviously depend on photolysis wavelength, the variations are not large [15], and the shapes of all the rotational distributions are similar. Thus, the relative intensities of the plotted LIF signals approximately reflect the relative populations of the NO vibrational levels. In agreement with the 300 K absorption spectrum, the onset of signal in the  $\nu=0$  PHOFRY spectrum occurs at wavelengths below 400 nm, with bands peaking at 380 and 388 nm. These bands are absent in the  $\nu=1$  PHOFRY spectrum, confirming the vibrationally

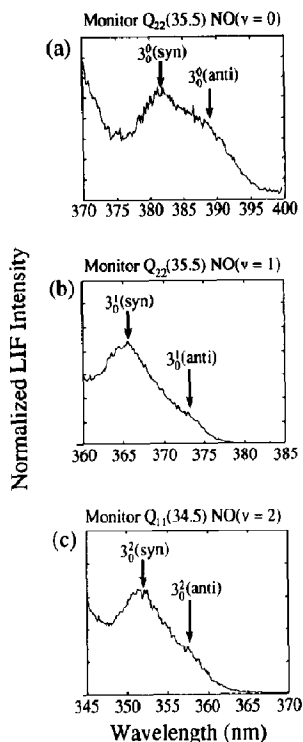


Fig. 3. State-specific PHOFRY spectra of methyl nitrite in the region of the  $3_0^n$  bands ( $n=0, 1, 2$ ) obtained by monitoring: (a) the  $Q_{22}(35.5)$  transition, (b) the  $Q_{22}(35.5)$  transition and (c) the  $Q_{11}(34.5)$  transition of the  $(0, 0)$ ,  $(1, 1)$  and  $(2, 2)$  bands of the NO  $\gamma$ -system, respectively. The suggested vibrational band assignments for the two rotamers are noted.

adiabatic dissociation mechanism in this region (i.e.  $n^* \rightarrow n$ ). In accord with the assignments of Tarte [21], we assign these two bands, which are shown more clearly in fig. 3a, to the  $S_1$  origins of the syn- (380 nm) and anti- (388 nm) systems. The spacing of these bands ( $\approx 510 \text{ cm}^{-1}$ ) is close to the ground state ONO bending frequency of the anti-rotamer ( $\approx 565 \text{ cm}^{-1}$ ); however, we reject the assignment of the 380 nm band as the first member of a progression in the ONO bending motion based on the unimodal, bell-shaped NO rotational distributions obtained following dissociation at that wavelength [22,29]. Had the ONO bending mode been excited, a rotational reflection model would predict bimodal NO rotational distributions [1,3]. The observed spacing of the origin bands implies that the anti-form is the more stable rotamer in the excited electronic state by  $\approx 290 \text{ cm}^{-1}$ . In contrast, the revised assignments [22–24]

imply a corresponding difference of  $\approx 1400 \text{ cm}^{-1}$ .

In a similar manner, and again consistent with the Tarte assignments [21], we assign the shoulders evident in the  $v=1$  and 2 PHOFRY spectra shown in figs. 3b and 3c to the anti-rotamer. The peaks at  $\approx 373$  and  $\approx 358 \text{ nm}$  are assigned to the  $3_0^1$  and  $3_0^2$  bands of the anti-rotamer, and the stronger features at  $\approx 364$  and  $\approx 351 \text{ nm}$  to the corresponding bands of the syn-rotamer. To extract more precise quantitative information regarding band positions, we fit the spectra to superimposed Gaussian functions using the ASYSTANT mathematics package. The peak positions determined from these fits, as well as the vibrational spacings, are shown in table 1.

Further support for the Tarte assignments [21] is obtained from the dependence of the observed shapes of the spectral features on the monitored NO rotational level. In fig. 4 are displayed four PHOFRY spectra in the region of the  $S_1$  origins of the syn- and anti-rotamers obtained by monitoring selected NO ( $v=0$ ) rotational levels. While the bandwidths and peak positions do not appear to significantly change with monitored rotational level, the relative intensities of the syn- and anti-bands vary. These changes in relative intensities presumably arise from slight difference in the NO rotational distributions following excitation into these two bands. REMPI spectra of the NO fragment have been obtained by Hippler et al., at photolysis wavelengths of 380 and 387 nm [22,29]; however, the rotational distribu-

Table 1

Band positions in the methyl nitrite  $S_1 \leftarrow S_0$  absorption system determined from Gaussian functional fits to the PHOFRY spectra obtained in this work <sup>a)</sup>

Band assignment	Rotamer	Energy ( $\text{cm}^{-1}$ )	$\Delta\nu$ ( $\text{cm}^{-1}$ )
$3_0^0$	anti	25802	–
$3_0^1$		26803	1000
$3_0^2$		27886	1083
$3_0^0$	syn	26313	–
$3_0^1$		27395	1081
$3_0^2$		28472	1077

<sup>a)</sup> These fits were obtained by optimization of superimposed Gaussian profiles. While the fits may not represent global minima, fit procedures beginning from randomly selected parameters yielded a variance in the final converged values ( $R^2 > 0.9969$ ) of  $< 0.01\%$ .

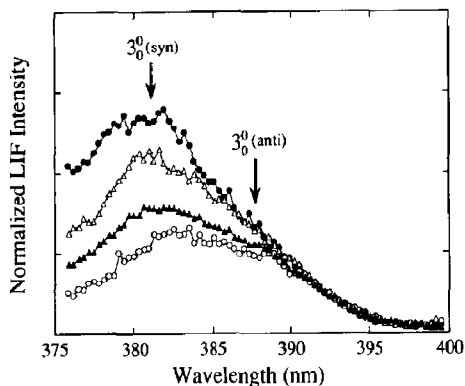


Fig. 4. Four state-specific PHOFRY spectra of methyl nitrite in the region of the  $S_1$  origins obtained by monitoring the ( $\circ$ )  $Q_{22}(35.5)$ , ( $\blacktriangle$ )  $Q_{22}(30.5)$ , ( $\triangle$ )  $Q_{11}(37.5)$  and ( $\bullet$ )  $Q_{11}(42.5)$  transitions in the  $(0, 0)$  band of the NO  $\gamma$ -system. The spectra were normalized in the "tail" region of the anti-rotamer origin band at 390–400 nm, since  $\text{NO}(v=0)$  rotational distributions in this region have not been reported.

tions have not been reported. We note that the absence of variations in the bandwidths with the monitored rotational level suggests that the dependence of the excited PES on the O–N=O angle in the Franck–Condon region is not strong. In contrast, in the case of FNO( $S_1$ ), the state-specific bandwidths change markedly with the monitored NO rotational level [26], in agreement with the calculated dependence of the PES on the FNO angle in the Franck–Condon region [1,3].

Also evident in the PHOFRY spectra displayed in figs. 2 and 3 are the large widths of the bands ( $\approx 500$ – $800 \text{ cm}^{-1}$  fwhm) which are not appreciably narrowed by jet-cooling. While the vibrational and torsional temperatures in our He expansion are unknown ( $T_{\text{rot}} < 10 \text{ K}$  by analogy with  $\text{NO}_2$  [30]), it is unlikely that these widths are dominated by inhomogeneous broadening, since the NO stretching vibration is the predominant Franck–Condon active mode [5,13]. The primary contribution to the observed widths must be lifetime broadening. If determined solely by lifetime broadening, the widths of the features in the PHOFRY spectra correspond to lifetimes  $< 10 \text{ fs}$ . These lifetimes are much shorter than the 200–300 fs lifetimes predicted by dynamical calculations on a PES that neglects the internal motions in the  $\text{CH}_3\text{O}$  moiety [13]. The calculations

show many recurrences in the NO stretch, whereas the experimental widths correspond to a single recurrence. We note, however, that since the contributions of inhomogeneous broadening to the observed widths are unknown and the bands are partially overlapped, the extraction of more exact lifetimes from these features must be approached with caution.

It is also intriguing to compare the lifetimes inferred from the observed absorption features with those estimated from the observed anisotropy parameters,  $\beta$ . Docker et al. have estimated dissociation lifetimes into all the observed NO vibrational levels following excitation into the syn-rotamer  $3_0^0$  band at  $\approx 350.8 \text{ nm}$ . They obtained  $\beta = -0.54$ ,  $-0.82$  and  $-0.95$  for  $v=0$ , 1, and 2, respectively. (The limiting value for the perpendicular transition is  $\beta = -1.0$ ). By using a quasi-diatomic model which also accounted for parent rotation, they reported lifetimes of  $320 \pm 100$ ,  $120 \pm 50$  and  $0$ – $50 \text{ fs}$  for  $v=0$ , 1, and 2, respectively [17]. These lifetimes should have resulted in a considerable narrowing of the state-specific linewidths when monitoring NO in  $v=0$  and 1 as compared with  $v=2$ . Such narrowing is not observed experimentally, and in fact a slight broadening is observed for the  $v=1$  linewidth compared to that observed when monitoring  $v=2$ . Thus, the decrease in  $\beta$  with decreasing  $v$  is not associated with an increase in lifetime and may show the influence of more subtle factors, such as out-of-plane motions and increased exit-channel interactions involving other parent vibrational modes in the non-adiabatic channels. For example, based on the measured NO state distributions at a fixed photolysis energy [16,17,25], it appears that both the relative fragment translational energy and the internal energy of the  $\text{CH}_3\text{O}$  fragment increase as the NO vibrational level decreases, since the NO rotational energy stays approximately constant. This increase may contribute to the decrease in  $\beta$ . In addition, the nonadiabatic transitions that result in the formation of NO in  $v=0$  and 1 may be promoted by out-of-plane motions which tend to reduce  $\beta$ . Thus, the lifetime inferred from the  $\beta$  value obtained when monitoring the adiabatic channel (i.e.  $\text{NO}(v=2)$ ) may be closer to the true photodissociation lifetime than the values obtained from the nonadiabatic channels. The former value is in good agreement with the lifetime in-

ferred from our observed linewidths.

We note that our results support the propensity for photodissociation via the nonadiabatic channel (i.e.  $n^* \rightarrow n-1$  when  $n^* > 0$ ). When exciting in the  $3_0^0$  region, only  $\text{NO}(v=0)$  is observed. However, when exciting in the  $3_0^1$  and  $3_0^2$  bands, the largest contributions to the partial cross sections are from  $\text{NO } v=0$  and 1, respectively, in agreement with both previous experimental results [15] and the calculations [13] for the syn-rotamer. The recently reported results on the  $\text{NO}$  vibrational distributions following 355 nm photolysis of jet-cooled samples also support the predominance of the nonadiabatic channels [22,23]. According to the Tarte assignments [21], and as evident from fig. 3, excitation at 355 nm preferentially excites the  $3_0^2$  bands of both the syn- and anti-rotamers. Therefore, the expected vibrational population maximum assuming a predominantly nonadiabatic dissociation mechanism [5] is at  $v < 2$ , consistent with the distributions obtained at 300 K [10,25] and under jet-cooled conditions [24].

#### 4. Conclusions

We have used state-specific PHOFRY spectra to probe the dissociation dynamics of jet-cooled methyl nitrite following one-photon excitation to the  $S_1$  surface. The spectra of the  $S_1 \leftarrow S_0$  system show distinct features at 380 and 388 nm and support the assignments of these bands by Tarte to the  $3_0^0$  transitions of the syn- and anti-rotamers, respectively [21]. The peaks have widths of  $500\text{--}800 \text{ cm}^{-1}$  and are not substantially narrowed compared to the 300 K absorption spectrum, suggesting that the dominant contribution to the observed linewidths is lifetime broadening. The observed linewidths are considerably narrower than predicted by dynamical calculations on a PES that freezes the internal motions of the methoxy moiety. We also find that vibrationally nonadiabatic predissociation on  $S_1$  is indeed the predominant decay mechanism. Finally, the widths of the spectra features show no strong dependence on the monitored rotational level over the range  $J=30.5\text{--}42.5$ , suggesting that the excited potential energy surface depends only weakly on the  $\text{ON}=\text{O}$  angle.

#### Acknowledgement

The authors wish to thank Dylan Stewart for assistance in methyl nitrite synthesis and purification and H. Floyd Davis for useful discussions and for critical reading of the manuscript. This research has been supported by NSF under Grants Nos. CHE9023632 and CHE9104248.

#### References

- [1] R. Schinke, *Photodissociation dynamics*, (Cambridge Univ. Press, Cambridge, 1993), and references therein.
- [2] H. Reisler and C. Wittig, in: *Molecular photodissociation dynamics*, eds. M.N.R. Ashfold and J.E. Baggott (Royal Society of Chemistry, London, 1987), and references therein.
- [3] J.R. Huber and R. Schinke, *J. Phys. Chem.* 97 (1993) 3463, and references therein.
- [4] U. Brühlmann, M. Dubs and J.R. Huber, *J. Chem. Phys.* 86 (1987) 1249.
- [5] S. Hennig, V. Engel, R. Schinke, M. Nonella and J.R. Huber, *J. Chem. Phys.* 87 (1987) 3522; M. Nonella, J.R. Huber, A. Untch and R. Schinke, *J. Chem. Phys.* 91 (1989) 194.
- [6] A. Tickton and J.R. Huber, *Chem. Phys. Letters* 156 (1989) 372.
- [7] B.A. Keller, P. Felder and J.R. Huber, *Chem. Phys. Letters* 124 (1986) 135.
- [8] F. Lahmani, C. Lardeux and D. Solgadi, *Chem. Phys. Letters* 129 (1986) 24.
- [9] F. Lahmani, C. Lardeux and D. Solgadi, *Chem. Phys. Letters* 102 (1983) 523.
- [10] O. Benoist D'Azy, F. Lahmani, C. Lardeux and D. Solgadi, *Chem. Phys.* 94 (1985) 247.
- [11] M. Nonella and J.R. Huber, *Chem. Phys. Letters* 131 (1986) 376.
- [12] B.A. Keller, P. Felder and J.R. Huber, *J. Phys. Chem.* 91 (1987) 1114.
- [13] A. Untch, K. Weide and R. Schinke, *Chem. Phys. Letters* 180 (1991) 265; R. Schinke, S. Hennig, A. Untch, M. Nonella and J.R. Huber, *J. Chem. Phys.* 91 (1989) 2016; V. Engel, R. Schinke, S. Hennig and H. Metiu, *J. Chem. Phys.* 92 (1990) 1.
- [14] H.U. Suter, U. Brühlmann and J.R. Huber, *Chem. Phys. Letters* 171 (1990) 63.
- [15] U. Brühlmann and J.R. Huber, *Chem. Phys. Letters* 143 (1988) 199.
- [16] E. Kades, M. Rosslein, U. Brühlmann and J.R. Huber, *J. Phys. Chem.* 97 (1993) 989.

- [17] M.P. Docker, A. Ticktin, U. Brühlmann and J.R. Huber, *J. Chem. Soc. Faraday Trans.* 85 (1989) 1169.
- [18] B.J. van der Veken, R. Maas, G.A. Guirgis, H.D. Stidham, T.G. Sheehan and J.R. Durig, *J. Phys. Chem.* 94 (1990) 4029.
- [19] P. Felder and Hs.H. Günthard, *Chem. Phys.* 71 (1982) 9.
- [20] P. Felder, T.-K. Ha, A.M. Dwivedi and Hs.H. Günthard, *Spectrochim. Acta* 37A (1981) 337.
- [21] P. Tarte, *J. Chem. Phys.* 20 (1952) 1570.
- [22] M. Hippler, M.R.S. McCoustra and J. Pfab, *Chem. Phys. Letters* 198 (1992) 168.
- [23] M. Hippler and J. Pfab, *J. Chem. Soc. Faraday Trans.* 88 (1992) 2109.
- [24] M.R.S. McCoustra, M. Hippler and J. Pfab, *Chem. Phys. Letters* 200 (1992) 451.
- [25] C.G. Atkins and G. Hancock, *Laser Chem.* 9 (1988) 195.
- [26] J. Brandon, S.A. Reid, D.C. Robie and H. Reisler, *J. Chem. Phys.* 97 (1992) 5246.
- [27] C.X.W. Qian, A. Ogai, L. Iwata and H. Reisler, *J. Chem. Phys.* 92 (1990) 4296.
- [28] A.H. Blatt, *Organic synthesis, collection*, Vol. 2 (Wiley, New York, 1969) p. 363.
- [29] M. Hippler, F.A.H. Al-Janabi and J. Pfab, *Chem. Phys. Letters* 192 (1992) 173.
- [30] M. Hunter, S.A. Reid, D.C. Robie and H. Reisler, *J. Chem. Phys.*, in press.